

Partitioning of ABA into Bilayers of Di-Saturated Phosphatidylcholines as Measured by DSC

Michael Katzer and William Stillwell

Department of Biology, Indiana University-Purdue University at Indianapolis, Indianapolis, Indiana 46202

ABSTRACT Using differential scanning calorimetry, we have investigated partitioning of the plant hormone abscisic acid into a homologous series of di-saturated phosphatidylcholines increasing in chain length from C₁₄ to C₁₉. Partition coefficients calculated from the shift in T_m range from 1280 for DiC₁₄PC to 480 for DiC₁₉PC. The free energy of transfer is chain-length independent with a value of $\Delta G = -17.4$ kJ/mol and an enthalpic contribution of $\Delta H = -22.6$ kJ/mol. The low net entropic contribution of $-\Delta S = -5.2$ J/mol agrees with the concept of the bilayer effect, but differs from that of the entropy-driven classic hydrophobic effect valid for partitioning between bulk solvents. Preferential location of the hormone in the outer region of the membrane is indicated by characteristic changes in the transition profiles and by comparison with partitioning into organic solvents whose dielectric constants model the interior and exterior regions of the bilayer. Differences in partitioning and surface pK_a between the biologically active *ct*-ABA and the inactive *tt*-isomer are discussed for biological relevance.

INTRODUCTION

Plasma membranes are complex barriers that separate the cell's interior from the extracellular medium. It is here that the uptake and loss of organic and inorganic solutes occur, thereby defining the osmotic properties of cells, generating membrane potentials and contributing to the general homeostasis that helps maintain cellular functions. The nonpolar interior of membranes provides the major barrier to transmembrane diffusion as well as being an appropriate solvent for membrane proteins (Lee et al., 1995). Of particular interest here is the amphipathic plant hormone abscisic acid (ABA). The hydrophobic nature of amphipathic solutes facilitates their partitioning into membranes (Gennis, 1989). Solute permeability is determined by the magnitude of membrane/water partition coefficients and is effected by both solute structure and membrane composition (Sarmiento et al., 1993, Finkelstein, 1976, Diamond and Katz, 1974, Xiang and Anderson, 1994). Not only does the membrane dictate total solute permeability, but the solute likewise influences the structural and physical properties of the membrane (Huang and McIntosh, 1997).

Membrane partitioning has been interpreted with regard to potential biological significance since the early work of

Overton (1901), who demonstrated a correlation between the anesthetic potency of narcotics and their partition coefficients between oil and water. More recently, Rowe et al. (1998) emphasized the importance of the thermodynamic state of membranes as a function of lipid composition, temperature, and dissolved solutes as a critical membrane property by investigating the effect of *n*-alcohols on model membranes.

To date, the majority of solute/bilayer investigations have focused on either straight chain amphipathic compounds as model systems to elaborate the physico-chemical mechanisms by which bilayer properties are modified (Lohner, 1991), or local anesthetics (Cantor, 1997) and drugs, which are not produced by the effected cells themselves, but instead are administered for medical or stimulatory purposes. Far fewer studies have been directed toward endogenous compounds produced by organisms as part of their normal biochemical and physiological activities. Plants in particular are exceptionally rich in bipolar products of their secondary metabolism. These include carotenes, flavonoids, and plant hormones (Heldt, 1997), many of which can be expected to accumulate inside membranes and thereby affect their state.

Several investigations with both natural and phospholipid membrane systems have shown the plant hormones auxin, gibberellin, and ABA can affect membrane properties (Burner et al., 1993, Shripathi et al., 1997). For example, Daeter and Hartung (1993) found that ABA crosses epidermal cell membranes passively, therefore requiring the hormone to be integrated into bilayers. Increases in conductivity and permeability to ions and solutes (Stillwell and Hester, 1984), and modification of membrane fluidity as well as induction of membrane fusion (Stillwell et al., 1988a) under the influence of ABA, have been indicated as well. Although attempts to identify a proteinaceous ABA receptor have been futile so far (Assmann and Shimazaki, 1999), the lipid phase-directed effects of ABA have been interpreted to be of potential biological significance (Stillwell and Hester, 1984, Harkers et al., 1985).

Submitted September 28, 2001, and accepted for publication July 26, 2002.

Address reprint requests to Dr. William Stillwell, Indiana University-Purdue University at Indianapolis, 723 W. Michigan St., Indianapolis, IN 46202-5132. Tel.: 317-274-0580; Fax: 317-274-2846; E-mail: wstillwell@iupui.edu.

Abbreviations used: *ct*-ABA, 2,4-*cis-trans* abscisic acid; *tt*-ABA, 2,4-*trans-trans* abscisic acid; DiC₁₄PC, dimyristoyl phosphatidylcholine; DiC₁₅PC, dipentadecanoyl phosphatidylcholine; DiC₁₆PC, dipalmitoyl phosphatidylcholine; DiC₁₇PC, diheptadecanoyl phosphatidylcholine; DiC₁₈PC, distearoyl phosphatidylcholine; DiC₁₉PC, dinonadecanoyl phosphatidylcholine; *DK*, dielectric constant; ΔG , free energy (of transfer); ΔH , enthalpy (of transfer); ΔS , entropy (of transfer); CU, cooperativity unit; P_m , partition coefficient; *n*, fatty acyl chain length (number of carbon atoms).

© 2003 by the Biophysical Society

0006-3495/03/01/314/12 \$2.00

So far, the biophysical investigations have provided little information on the magnitude, or the molecular and physical details of the interaction between ABA and the lipids that constitute the bilayer. In the present investigation, we use the nonperturbing technique of differential scanning calorimetry (DSC) to probe the interaction of ABA with membranes. By applying the model of the freezing point depression of solvents by solutes to lipid phase transitions and bilayers, DSC allows one to establish the concentration dependence of the uptake of ABA into membranes as well as to calculate the partition coefficients from which the concentration of the hormone inside bilayers can be obtained (Lee, 1977). Using phase transitions of several di-saturated phosphatidylcholines of increasing chain length spaced over a range of temperatures, one can obtain, by routine thermodynamic calculations, the free energy, enthalpy, and entropy of solute partitioning (Atkins, 1990; Rowe, 1983). Contrary to other routine techniques for quantification of solute partitioning, DSC further provides information on the location of ABA within the membranes from characteristic changes in the transition profiles. Possible biological implications of these findings are discussed by comparing the effects of the biologically active *ct*-ABA isomer with the inactive *tt*-ABA form, which differ in their *in-vivo* potency by a factor of 50–100 (Addicott, 1983). As only the protonated species HABA partitions into membranes (Stillwell et al., 1988b), we further determined surface *pKa* values for both isomers. Differences are discussed within the background of data on a natural pH range of 5.5 (Pfanzen and Dietz, 1987) to 7.5 (Slovik and Hartung, 1992) in leaf cell walls. Subsequent studies will deal with the effect of unsaturation, sterol content, lipid miscibility and domain structure on partitioning of ABA into membranes as well as possible effects of the hormone on thermodynamic and structural properties of bilayers.

MATERIALS AND METHODS

Materials

All phosphatidylcholines (PCs) were purchased from Avanti Polar Lipids (Alabaster, AL) and used without further purification, as occasional checks by TLC and DSC scans (Mabrey and Sturtevant, 1976) did not indicate impurities. *ct*-ABA was from Fluka (Milwaukee, WI), whereas *tt*-ABA was purified by high performance liquid chromatography (HPLC) from a mixture of *ct*- and *tt*-ABA using published protocols (Mapelli and Rocchi, 1983) or was purchased from Sigma (St. Louis, MO). Water was deionized, glass distilled and further purified via a Milli-Q system (Millipore, Bedford, MA) before use.

Sample preparation

All lipids were weighed into glass tubes from stock solutions in chloroform, evaporated to dryness under nitrogen, and further dried overnight under vacuum, over P₂O₅. For most experiments, hydration of the lipids was done 7°K above their respective main phase transition temperature in 200 mM KCl and 20 mM acetic acid buffered with arginine to pH 4.8, ABA was

dissolved at 3 mM in alkaline pH from dry powder, adjusted to pH 4.8 and diluted to the indicated concentrations with buffer. After hydration, samples were passed five times through their phase transitions using liquid nitrogen and hot water. Approximately 400 μ l solutions with a final lipid concentration of 4 mg/ml (~5.5 mM, depending on the MW of the respective lipid) were dispensed into the stainless steel ampoules of the calorimeter and degassed before the scan. DSC scans requiring quantities of ABA beyond its reported aqueous solubility limit (3 mM) were prepared by adding ABA in excess of 3 mM directly from 100-mM stock solutions in EtOH to the lipid in chloroform, after which the samples were dried and hydrated as usual in presence of 3 mM ABA dissolved in buffer. The final concentration of ABA is indicated as the one that would have been obtained from complete solubility of ABA in the aqueous phase. After hydration for 1 h, these samples were sonicated for 10 s in a water bath sonicator to ease dispersal before the usual passage through nitrogen/hot water. This protocol guaranteed maximum uptake and dispersal of ABA into the lipid bilayers, as can be seen from the fact that the decrease in *T_m* of the lipids is linear beyond the aqueous solubility limit of ABA (3 mM). Controls with multilamellar vesicles (MLVs) of classic onion-skin structure prepared by a similar protocol, but without the freezing/heating step, and instead subjected to several passages through *T_m* inside the DSC, produced the same results within experimental error. We therefore decided to routinely use the first protocol that includes freezing/thawing and employs the same steps in preparing MLVs for extrusion. This procedure allows for better solute exposure to the looser stacked lipid layers. As the total amount of the hormone dissolved in the lipid bilayer is small compared to the total amount of ABA present, uptake of ABA into the bilayers was not limited by availability of ABA in either concentration range below or beyond 3 mM. The value of the partition coefficients was further controlled by centrifuging samples of the final MLV suspensions and comparing the ABA concentration in the supernatant with that of buffer before lipid addition. Where necessary, the corrected concentration of ABA within the aqueous phase after partitioning was used for computation of partition coefficients. Deviations in ABA concentration within the buffer before and after partitioning were found to be small, and only measurable for the highest partition coefficients with DiC₁₄PC, DiC₁₅PC, and DiC₁₆PC. The lower partition coefficients of lipids with longer fatty acid chains did not result in measurable depletion of the buffer with ABA.

Calorimetry

Measurements were carried out on a Model 4207 Hart Scientific Microcalorimeter (Calorimetry Sciences, Provo, UT) at a scan rate of 5°K/h. All samples were passed once through the lipid's main transition inside the instrument and were then equilibrated 15°K below their pretransition temperatures for periods increasing in duration with chain length (minimum of 1.5 h) before start of the scan. Consecutive heating and cooling scans were separated by 1 h of sample equilibration at a temperature 10°K above the main transition of the respective lipid. Thermograms were analyzed using software provided by the manufacturer.

Calculation of partition coefficients

The following formula has been employed for calculation of partition coefficients from plots of the temperature shift of the main transition temperature of lipids versus aqueous concentration of solute (see Fig. 4).

$$P = \frac{-\Delta H_0}{RT_0^2} \left(\frac{-\Delta T}{X_{s,sol}} \right),$$

where *P* is the bilayer/water partition coefficient, *X_{s,sol}* is the mol fraction of solute in solution, ΔT is the temperature shift at the given mol fraction of solute, *R* is the gas constant, and *T₀* and ΔH_0 are the midpoint and enthalpy of the lipid phase transition in the absence of solute. Derivation of the formula employed here can be found in the publications of Rowe (1983), Lee (1977), and Kamaya (et al., 1981), who reviewed and extended the

earlier work of Hill (1974). It should be pointed out, however, that the depression of the melting temperature depends not so much on solute concentration within the liquid phase, but rather on the difference in ABA concentration between solid and liquid phases (Lee, 1977):

$$\Delta T \approx \frac{RT_o^2}{\Delta H_o} (X_{\text{solute}}^l - X_{\text{solute}}^g),$$

where X_{solute}^l is the solute concentration in the liquid phase, and X_{solute}^g the solute concentration in the solid phase. Partition coefficients obtained by this approach therefore have to be regarded as a lower limit, which underestimates the real value by the amount of solute partitioning into the solid phase below T_m . Although this theoretical model was originally derived for interaction of solutes with bulk solvents, further work by Rowe (et al., 1998, Fig. 5), shows near-perfect agreement between partition coefficients of *n*-alcohols into bilayers obtained by the method employed here and by isothermal titration calorimetry.

RESULTS

Fig. 1 shows ct-ABA (the biologically active isomer; see Walton, 1983), and its geometric isomer tt-ABA, compared

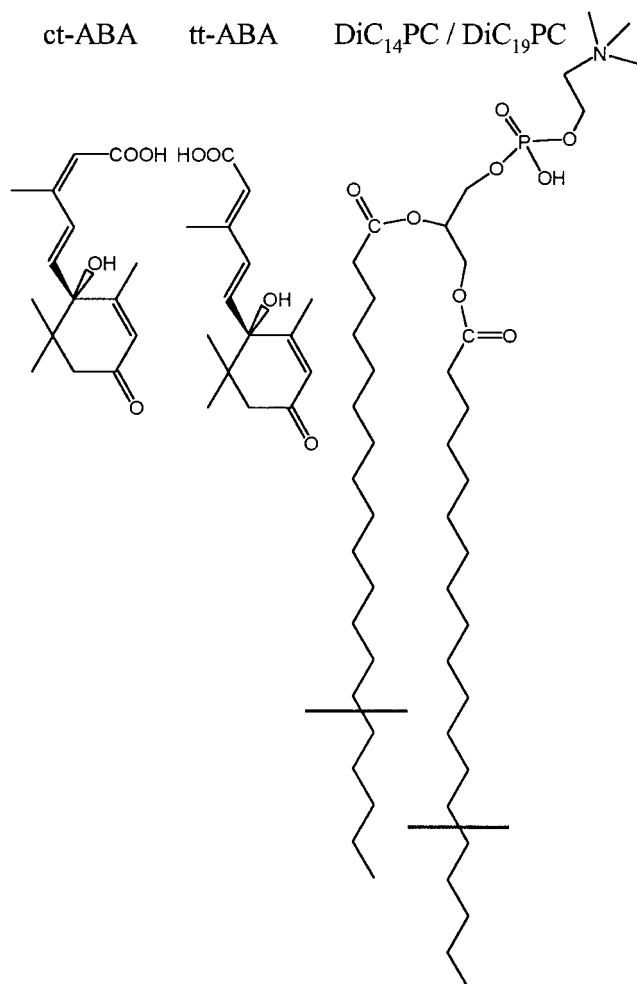


FIGURE 1 Structure of ct- and tt-ABA relative to the shortest and longest lipids used in this study, DiC₁₄PC and DiC₁₉PC. The lines across the fatty acid tails mark the length of DiC₁₄PC.

to the shortest (C₁₄) and longest (C₁₉) di-saturated phosphatidylcholines employed in these studies. ABA has approximately the same length as a fatty acyl chain of eight carbon atoms. Although the overall structures and physical properties are very similar, the two ABA isomers exhibit large differences in their biological activity. Fig. 1 does, however, reveal subtle but likely significant structural differences: The tt-isomer is slightly longer than the ct-isomer, resulting in a larger separation between the carboxyl and hydroxyl groups than for the ct-form.

Fig. 2 compares the main phase transitions of all six lipids used in these experiments in absence (*solid lines*) and in the presence (*dashed lines*) of 3 mM ct-ABA. In absence of the hormone, the transition temperature and enthalpy increase with acyl chain length, whereas the cooperativity (indicated by the relative peak width) of the chain melting process decreases. A closer look at selected lipids (Fig. 3) shows acyl chain-dependent changes of the transition profiles in response to ABA partitioning into the membrane. DiC₁₆PC is considered here as a standard lipid, displaying all common characteristics of the ABA-lipid interactions, but missing some of the specific features noted for lipids with shorter or longer fatty acyl tails. We therefore begin by describing the effect of ABA on DiC₁₆PC as the general case, before proceeding with PCs of shorter or longer acyl chains. It should be noted here that only the protonated form of either ABA isomer interacts with bilayers. This fact has been documented before (Stillwell et al., 1988) and will be outlined in more detail further below in the measurement of the surface *pKa*.

DiC₁₆PC

As can be seen in Fig. 2 and in more detail in Fig. 3 C, ct-ABA decreases the T_m of DiC₁₆PC and broadens the phase transition. This is consistent with theoretical models that explain a decrease in transition midpoint with partitioning of solutes into the liquid phase, analogous to the effect of

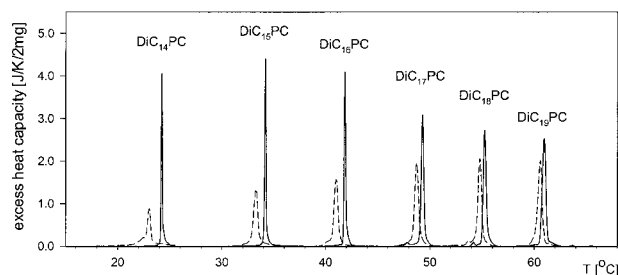


FIGURE 2 The main phase transitions (T_m) of DiC₁₄PC, DiC₁₅PC, DiC₁₆PC, DiC₁₇PC, DiC₁₈PC, and DiC₁₉PC in absence of ct-ABA (*solid lines*) and presence of 3 mM ct-ABA (*dashed lines*). Note that the cooperativity (i.e., width of the transition) is independent of the enthalpy of the transition, and that although the latter increases with chain length, the former decreases (Mabrey and Sturtevant, 1976).

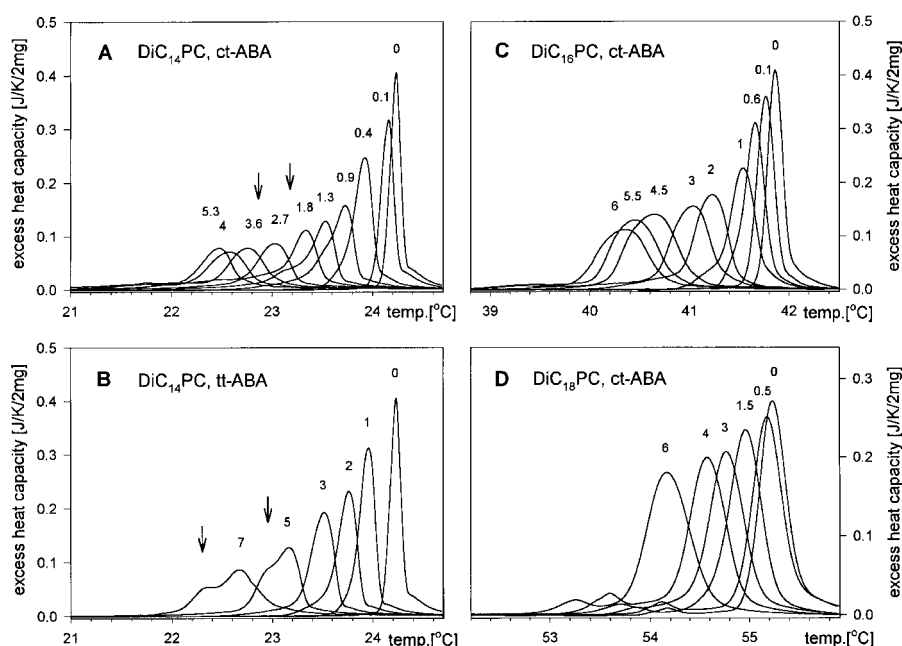


FIGURE 3 Heating scans of (A) DiC₁₄PC + ct-ABA, (B) DiC₁₄PC + tt-ABA, (C) DiC₁₆PC + ct-ABA, and (D) DiC₁₈PC + ct-ABA. For clarity of presentation, only selected scans are shown. The numbers on top of the peaks indicate the ABA concentration [mM] used and allows for a comparison of the molecular ratio of ABA to lipid (lipid concentration is 4 mg/ml, which corresponds approximately to 5.5 mM (DPPC), depending on the MW of the lipid in question). The molar ratios of membrane-dissolved ABA to lipid for a 1-mM aqueous solution of ABA (see Table 1) are as follows: DMPC, ct-ABA:1/60, DMPC, tt-ABA:1/144; DPPC, ct-ABA:1/80; and DSPC, ct-ABA:1/130. The arrows point at the location of the shoulders as discussed in the text for DMPC.

dissolved substances on the freezing point of water (Lee, 1977). Broadening of the phase transitions is a consequence of the reduction in cooperativity of the transition, which represents the parameter of phase transitions that is most sensitive to the presence of foreign substances (i.e., ABA) partitioning between the lipids (Mabrey and Sturtevant, 1976). As holds for the other lipids employed, the enthalpy of the main transition does not change with ABA concentration (typically less than 5% deviation to either side of the value in absence of ABA, data not shown), indicating that the interaction of the phospholipids with each other is not reduced much by the hormone. In contrast, the measured reduction in T_m and the widening of the phase transition as a result of solute uptake is frequently interpreted to reflect an increase in membrane fluidity. Also observed are lipid pretransitions shifted toward lower temperatures (data not shown), indicating some partitioning of ABA into the ripple phase. This would be in agreement with reports describing the ripple phase as containing defects or of having partial liquid character (Muller et al., 1986), which explains the larger uptake of solutes into the P_{β}' phase compared to the L_{β}' phase of PCs.

DiC₁₄PC, DiC₁₅PC, and DiC₁₆PC

These three lipids, although exhibiting a similar response to abscisic acid, differ from the longer chain lipids used in the present study in their lack of a submain transition, (DiC₁₄PC, Fig. 3 A and DiC₁₆PC, Fig. 3 C; DiC₁₅PC, not shown). T_m decreases with ct-ABA concentration, and the transition broadens. The pretransition is already obliterated at low ct-ABA concentrations. The transition profiles of all three lipids are asymmetric and display a lower temperature shoulder,

the position and height of which (relative to the main peak) is ct-ABA-concentration dependent. This shoulder is more pronounced in cooling compared to heating scans (data not shown) and is reduced in magnitude with longer PC acyl chains. The slightly longer (see Fig. 1) and biologically inactive tt-ABA induces an even more pronounced shoulder in the main transition of DiC₁₄PC (Fig. 3 B) than does the ct-isomer (Fig. 3 A). The enthalpy of the main transitions of all three lipids remains unchanged over the investigated ABA concentration range, which indicates only minor hormone-induced disruptions of the interaction between the PC molecules.

DiC₁₇PC, DiC₁₈PC, and DiC₁₉PC

The main transition of these lipids (data only shown for DiC₁₈PC, Fig. 3 D) exhibits a concentration-dependent change similar to that noted for the shorter chain lipids, i.e., a linear decrease in T_m and a broadening of the transition due to reduced cooperativity. DiC₁₇PC, DiC₁₈PC, and DiC₁₉PC differ, however, from the shorter lipids investigated here by having a submain transition as described by Jorgensen (1995) and Pressl (et al., 1997). Addition of ABA does not seem to effect the enthalpy of this transition, but does reduce the temperature difference between the submain transition and the main transition from 1.05 to 0.6°C. The precise nature and origin of the submain transition is largely unclear, although Pressl (et al., 1997) detected a "rearrangement of the hydrocarbon chain packaging (of the rippled phase) and an onset of chain melting" over the temperature range using wide-angle x-ray diffraction. According to these authors, this suggests the coexistence of two distinct domains that are fluid or solid. Incorporation of ABA into the membrane in

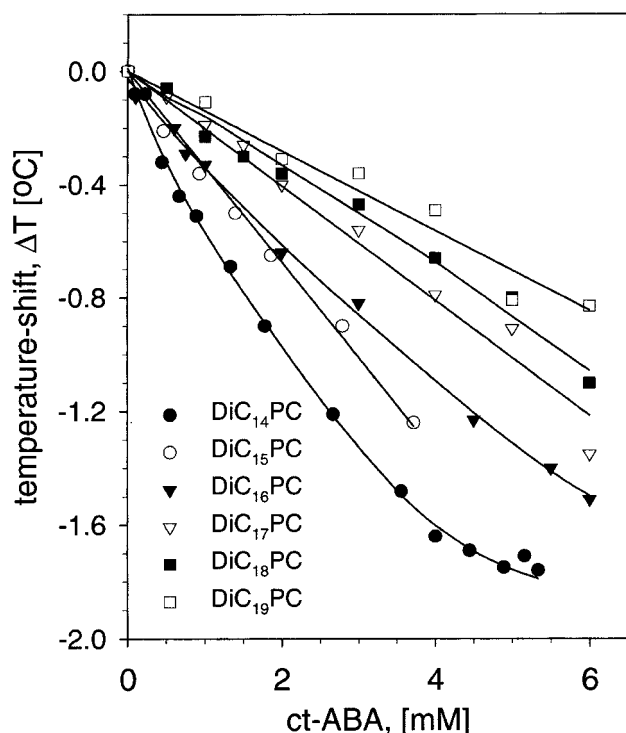


FIGURE 4 The ct-ABA-concentration-dependent shift of the temperature midpoint of the main transition (T_m) for: DiC₁₄PC, DiC₁₅PC, DiC₁₆PC, DiC₁₇PC, DiC₁₈PC, and DiC₁₉PC bilayers. The shift in T_m is reported as the change of the transition temperature relative to the value in absence of ABA.

the phase between the submain and main transitions (denoted “rippled phase II” by Pressl et al., 1997) seem to induce an earlier transition to the liquid phase at a relatively lower temperature as seen from the narrowing of the temperature range of this phase. This can be interpreted as favoring chain melting and a destabilization of ripple phase II, possibly by facilitating the formation of domains of molten or liquid-like lipid. As with the shorter chain lipids, no change in the enthalpy of the main transition was detected for up to 6 mM ct-ABA.

Chain length dependence of T_m -shifts and partition coefficients

Fig. 4 compares the ABA-concentration-dependent reduction in T_m of the main transition for the various PCs used here. As reviewed by Lee (1977), the decrease in the lipid transition temperature follows the same physico-chemical laws as the freezing point depression of water and is driven by increased concentration of solute in the liquid phase. More specifically for the experiments presented here, the observed ABA-induced decrease in T_m reflects the difference in concentration of the hormone between the ripple versus the liquid crystalline phase.

Possible partitioning or strong interaction of ABA with the

solid phase would lead to an underestimation of the partition coefficient because ΔT would be reduced in magnitude. In the present investigation, we compared the buffer concentration of ABA before and after addition of lipid and partitioning into MLVs, which allowed us to calculate partition coefficients also from the depletion of ABA from the aqueous phase due to membrane partitioning. The values (data not shown) indicate only a minor underestimation of the magnitude of the partition coefficients derived via Hill’s method, and consequently indicate a negligible interaction of ABA with the gel phase. The slopes of the curves in Fig. 4 therefore represent differences in the partitioning of ABA into the lipids, which is lowest for DiC₁₉PC and increases toward the shorter DiC₁₄PC. It should be noted here that the slopes for the lipids with longer chains are linear with increasing ct-ABA, whereas the graph of DiC₁₄PC is non-linear beyond 3 mM ct-ABA. This likely indicates that membranes made from the shorter lipids are close to ct-ABA saturation.

Partition coefficients between water and lipid bilayers have been obtained from the temperature shift versus solute concentration plots in Fig. 4 for ct-ABA using the equation given in Methods. As this formalism holds only for concentrations well below the aqueous solubility limit of the solute, we used only the portion of the curves in Fig. 4 up to 1 mM ABA. Fig. 5 *A* plots the partition coefficients as a function of PC acyl chain length, and Table 1 presents the actual values of the parameters obtained from the curves. P decreases from 1280 for DiC₁₄PC to 480 for DiC₁₉PC, reflecting changes in the slopes of the T_m versus ct-ABA-concentration curves. R_{1mM} in Table 1 is the mol ratio of ABA/PC, calculated on the basis of the derived partition coefficients for a concentration of 1 mM ABA in solution. The free energies of ABA transfer in Table 1 have been calculated using $\Delta G_t = -RT \ln P$, whereas the enthalpy of transfer, ΔH_t was obtained from the slope of the Van’t Hoff plot shown in Fig. 5 *B*. The relationship $\Delta G_t = \Delta H_t - T\Delta S_t$

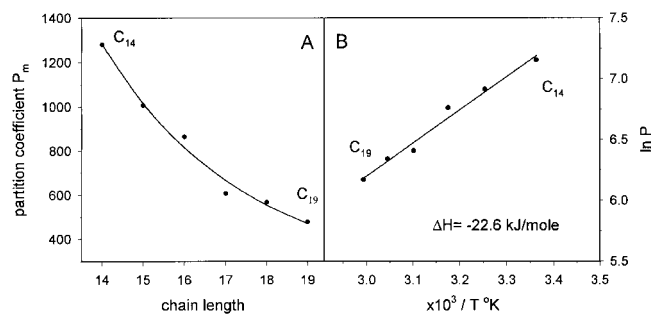


FIGURE 5 (*A*) Chain-length dependence of the partition coefficients (P_m) for ct-ABA reported in Table 1. (*B*) Van’t Hoff Plot. The slope of the straight line obtained from plotting $\ln P_m$ over the inverse of the temperature gives the enthalpy of transfer (-22.6 kJ/mol) for ct-ABA from aqueous to lipid phase. The solid circles connected by solid lines in both panels represent the curves fitted to the experimental partition coefficients from DiC₁₄PC to DiC₁₉PC bilayers.

TABLE 1 Partition coefficients (P) and thermodynamics of transfer (ΔG_t , ΔH_t , and ΔS_t) of ct-ABA (our data) into bilayers made from disaturated PCs with increasing chain length and transition temperature (T_m)

Chain length n :	C ₁₄	C ₁₅	C ₁₆	C ₁₇	C ₁₈	C ₁₉
T_m [°C]:	24.2	34.2	41.8	49.3	55.3	60.9
$\frac{100^\circ \Delta H}{RT_m^2}$:	2.86	3.59	3.69	4.50	4.59	5.16
ABA						
ΔT_m (1 mM):	−0.55	−0.35	−0.32	−0.19	−0.17	−0.13
P_m :	1280	1010	870	610	570	480
ΔG_t [kJ/mol]:	−17.7	−17.7	−17.5	−17.2	−17.3	−17.1
ΔH_t [kJ/mol]:	−22.6	−22.6	−22.6	−22.6	−22.6	−22.6
ΔS_t [J/Kmol]:	−16.6	−16.2	−16.3	−16.9	−16.3	−16.6
R_{imm} :	1/60	1/70	1/80	1/120	1/130	1/150

R_{imm} is the ratio of moles ct-ABA/mol PC inside the bilayers, and ΔT_m (1 mM) gives the temperature shift [°C] of the phase transition for a 1-mM concentration of ABA in buffer.



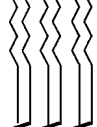

was then used to obtain the entropic contribution for the partition step. Values ~ -17.4 kJ/mol for the Gibbs free energy of transfer and -22.6 kJ/mol for the enthalpy of partitioning were obtained, denoting a decrease in free energy due to the entropic contribution by 5.2 kJ/mol. The transfer of ct-ABA from the aqueous phase to the membrane is therefore dominated by the enthalpy of transfer, and not by the entropic contribution, as might be expected on the basis of the classic hydrophobic effect (Tanford, 1980). Contained within the overall high value for the free energy of transfer is a slight chain-length dependence that decreases the magnitude of ΔG_t from -17.7 kJ/mol for DiC₁₄PC to -17.1 kJ/mol for DiC₁₉PC.

Location of ABA in membranes

Jain and co-workers (Jain and Wu, 1977) have developed a model that associates characteristic changes in lipid phase

transition profiles induced by various solutes with the location of the solute inside a bilayer. Applying this model to our DSC scans with ct-ABA (which show a simultaneous decrease of T_m and cooperativity) indicates the preferential location of the hormone in the upper methylene region from C₁ to C₈ of the fatty acyl chains (Table 2). This outward location for ABA is confirmed by comparing its partition coefficient into lipid bilayers with those obtained for partitioning into octanol and *n*-decane: The P value for octanol ($DK = 10$, *Handbook of Chemistry and Physics*, Lide, 2001) is 300, while for *n*-decane ($DK = 2$, *Handbook of Chemistry and Physics*, Lide, 2001) it is only 3.3. Estimates of the DK for the hydrocarbon core of membranes are ~ 2 and range between 10 and 30 for the headgroup region (Raudino and Mauzerall, 1986). Octanol and decane are therefore commonly used to model solute partitioning into regions of bilayers with corresponding DK s (Xiang et al., 1990). The ABA partition coefficient of 300 in octanol

TABLE 2 Summary on the data for the site of integration of ABA into bilayers

Model solvent	DK	Location Profile-type	T_m	ΔH_o	C.U.P.
Octanol: P_m : 300 DK : 10	10–30	 Headgroup D	New peak large shift in T_m	Final unchanged	Final unchanged
Decane: P_m : 3.3 DK : 2	2	 Glycerol backbone B	Shoulder on main peak	Shoulder increases with conc.	Decreases for shoulder
Lipid: DiC ₁₄ PC: P_m : 1140 DiC ₁₉ PC: P_m : 470	2 10–30	 C₂ to C₈, upper methylene area A	Decrease	Unchanged	Decrease
		 C ₉ to C ₁₆ , central hydrocarbon region C	Decrease	Unchanged	Unchanged

Adjacent to the diagram of a bilayer are shown the four different regions of the phospholipids with which solutes can interact (based on the model of Jain and Wu, 1977): *D*, the polar, hydrated headgroup; *B*, the glycerol backbone; *A*, the ordered chain region of the upper methylene area (C₂ to C₈); and *C*, the lower methylene area from C₉ to the end of the chains. Column 1 compares the partition coefficients of ABA into different model solvents and PCs, whereas column 2 gives estimated values for the DK of different regions of the bilayer (Raudino and Mauzerall, 1986). The columns on the right summarize the evidence for membrane location derived from the changes in the transition profiles based on models developed by Jain and Wu (1977). The changes found in our experiments are given in bold underlined print.

(Table 2) is closer to the values obtained for the PCs ($P = 1280$ to 480) than for *n*-decane ($P = 3.3$). This supports the outward location of the hormone in the bilayer and is consistent with the presence of three polar oxygens on ABA. We therefore suggest that ABA is largely excluded from the interior of the membrane. The absence of an ABA-induced change in the enthalpy of the main transition, which holds for DiC₁₄PC, DiC₁₆PC, and DiC₁₈PC, is typical for solutes residing in the outer portion of the bilayer (Jain and Wu, 1977; McElhaney, 1986). Together, the short length of ABA relative to the lipids (Fig. 1) and the DSC data on the external location of ABA within the bilayers predict that ABA cannot cause a major disruption in lipid packing beyond acyl chain carbon number 14. We have also noticed the presence of a shoulder on the lower temperature side of our DSC profiles that increases in intensity from DiC₁₆PC to DiC₁₄PC. Jain and Wu (1977) attribute these shoulders to an interaction between solute and the phospholipid glycerol backbone.

ct-ABA versus tt-ABA

ABA exists in two geometric isomers, ct-ABA and tt-ABA, of which only the ct-isomer shows significant biological activity (Walton, 1983). As the two isomers have very similar structures and physical properties, we next compared the effect that each isomer has on DiC₁₄PC bilayers using DSC. Both isomers reduce T_m and broaden the phase transition. Heating scans for DiC₁₄PC in the presence of tt-ABA are, however, distinguished by a more prominent lower temperature shoulder than were noted for the ct-isomer (Fig. 3 *B* compared to Fig. 3 *A*). Fig. 6 *B* further shows a difference between the isomers as higher quantities of

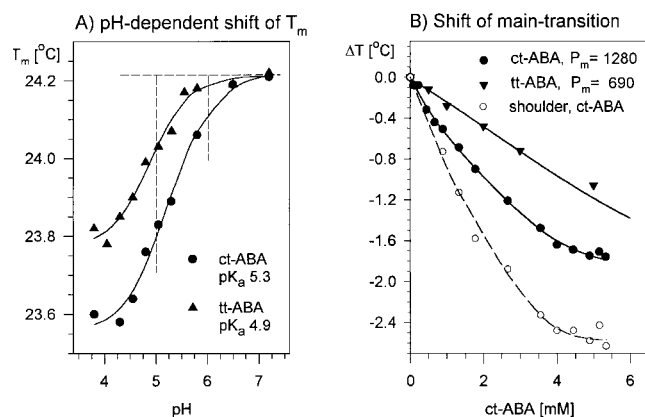


FIGURE 6 Comparison of ct- and tt-ABA on the thermotropic properties of DiC₁₄PC bilayers. (A) Effect of pH on the main transition temperature (T_m) at 1 mM ct- or tt-ABA. Surface pK_a values of 5.3 (ct-ABA) and 4.9 (tt-ABA) are determined from the sigmoidal plots as described in Materials and Methods. The dashed lines at 5 and 6 mM ABA demonstrate the increase in the ratio of surface concentration of ct- versus tt-ABA. (B) Comparison of the ct- or tt-ABA-concentration-dependent shift in T_m of the main phase transition of DiC₁₄PC. The dashed line shows the increasing temperature difference between the shoulder and the main peak for ct-ABA.

tt-ABA are required to achieve the same temperature shift than for ct-ABA. The pH-dependent shifts in T_m of a 1-mM solution of both isomers were used to determine the isomer's surface pK_a 's. The resulting sigmoidal fits shown in Fig. 6 *A* gives a pK_a of 5.3 for ct-ABA and 4.9 for the tt-isomer. The plot further demonstrates that only the protonated species affects the bilayers, in agreement with the findings of Burner (1993). Using Henderson-Hasselbalch, the measured difference in pK_a values translates into a lower concentration of protonated tt-ABA at the membrane surface compared to the ct-isomer present at the same subphase pH. Fig. 6 *A* shows that at low pH, when both isomers are fully protonated, ct-ABA exerts a larger effect on T_m than does tt-ABA. This is reflected in the partition coefficients and free energies of transfer of the two isomers (ct-ABA, $P = 1280$, $\Delta G_t = -17.7$ kJ/mol; and tt-ABA, $P = 690$, $\Delta G_t = -16.2$ kJ/mol).

DISCUSSION

The experiments presented here demonstrate the uptake into and effect on membranes of the plant hormone ct-ABA by monitoring its effect on the transition profiles of di-saturated PC bilayers using DSC. The degree of membrane interaction is quantified by deriving partition coefficients and the energetics of transfer of ABA from water into membranes from the ABA-induced shifts in the PC's T_m . Changes in the parameters of enthalpy, cooperativity, and midpoint temperature of the transition are combined to determine the hormone's location in membranes.

Effect of ABA on phase transitions

The effects of ct-ABA on phase transition of lipids, which are summarized in Fig. 2, are similar to the effects found by Bach (1986): a decrease in the midpoint temperature and cooperativity of the main phase transition of the lipids. The approach previously used by Bach (1986) is, however, limited by the use of high lipid concentrations, and therefore ABA concentrations, beyond the solubility of the hormone as required by the use of differential thermal analysis (DTA) equipment. In contrast, by employing high-sensitivity DSC, we can use millimolar lipid and ABA concentrations, which allows us to derive partition coefficients and characterize the energetics of the ABA-membrane interaction by including an evaluation of the chain-length dependence (and therefore temperature dependence) of the partitioning.

Partition coefficients and energetics of partitioning

The partition coefficients reported here are based on the approach of Hill (1974), which is an extension of the well-known depression of the solvent freezing point by solutes to the T_m of phospholipids. Measuring the "freezing" points of bilayers by DSC allows us simultaneously to obtain

information on the state of the membranes as well as the nature of the lipid-solute interaction from the transition profiles. Furthermore, as a scan is performed over a larger temperature range, information on solute partitioning into several different phases is obtainable from the associated transitions.

The method requires the use of mol fractions as the units for concentration (more precisely mol ratios, which in dilute solutions approximate mol fractions), which further allows for calculation of the free energy of transfer, but complicates comparison with plant physiological literature that relies on the classical use of molarities or better, molalities. The interested reader is referred to the publications of Diamond and Katz (1974) and Kamaya (et al., 1981) for simple formulas for interconversion of the different units and comparison with relevant publications.

Table 1 displays the values for ΔG_t , ΔH_t , and ΔS_t for transfer of ABA from water into PC bilayers of different chain lengths. ΔG_t was derived directly from the partition coefficients as described in Results, whereas the enthalpy was obtained from the Van't Hoff plot in Fig. 5 B by plotting values from a homologs series of phosphatidylcholines of increasing chain length. Although ΔG_t shows a small variation with acyl chain length, the values for ΔH_t do not change with either PC acyl chain length or temperature. This is in contrast to several other solutes such as ethanol, benzene, and *n*-hexane, whose free energy of transfer and partition coefficients increase significantly with acyl chain length and temperature (DeYoung and Dill, 1990; Rowe, 1983). Because $\Delta G_t = -RT \ln P$ and T_m increases with chain length from DiC₁₄PC to DiC₁₉PC, the nearly constant free energy of transfer of ABA therefore requires that the partition coefficients decrease simultaneously with T_m . Part of this can be explained by the nearly twofold increase in aqueous solubility of ABA from 20 to 50°C (data not shown). The chain-length dependence of partitioning depends, however, on several complex factors including lipid surface density (DeYoung and Dill, 1988, 1990), temperature, volume of the bilayer, and the steepness of the *DK* gradient normal to the bilayer surface, all of which vary with acyl chain length. It is therefore difficult to judge, only on the basis of our experiments only whether the small change in the energy of transfer relative to its overall high value is solely the result of underlying changes in solubility with temperature in either phase, or represents the effect of a hidden tendency for either an increase or decrease in membrane solubility of ABA with changes in acyl length.

Tanford (1980) has shown that the enthalpy of transfer for hydrocarbons and amphiphiles depends on temperature. This means that, in our experiments, such a variation is either small and hidden below variation of the data; that the applied model for computation of the enthalpy by itself is insufficient by assuming a linear relationship between $\ln P$ and the inverse of the temperature; or that the details of partitioning into interfacial assemblies like membranes contain determinants

that are missing in bulk solvents. Although the data points that compose the Van't Hoff plot in Fig. 5 B are derived from phosphatidylcholines of increasing chain length, they allow for a good linear fit. Enthalpic contributions to ΔG_t of transfer depend either on changes in intermolecular bonds between the solute and the solvent in either phase, or, as suggested by Wimley and White (1993), on dipolar interactions. However, dipolar interactions can be expected to vary with acyl chain length, as the slope of the polarity gradient from headgroup to the methylene ends of the lipid changes. No change in the site of membrane interaction would consequently imply only a slight change in the enthalpy of transfer with acyl chain length. To fully answer this question about why there is little change in the enthalpy of transfer of ABA with acyl length, more detailed investigations covering a larger temperature range would be required.

Comparing the relative contributions of enthalpy and entropy to the free energy of transfer shows that the membrane uptake of ABA is enthalpy-driven and therefore follows the features of either nonclassical hydrophobic partitioning (Seelig and Ganz, 1991), or what has been called the "bilayer effect" (Wimley and White, 1993). Hydrophobic partitioning attributes the low entropic contribution to rebinding of water released from the solute during transfer to the hydrocarbon surface and to increased disordering of the acyl chains. In contrast, the bilayer effect discussed by Wimley and White (1993) and based on indole partitioning, assumes that the contribution of the hydrophobic effect to the overall energetics of transfer is hidden below a low net entropic contribution reduced by the incomplete loss of hydration water from the solute located at the aqueous interface. In the case of ABA, the entropic contribution decreases the enthalpic component to the free energy of transfer by approximately -5.2 kJ/mol. This indicates a net decrease in entropy when ABA enters the lipid phase relative to the gain in entropy from release of surface-bound water upon exit from the aqueous phase. This loss in entropy could either be due to a net uptake of water into the bilayer, or to a decrease in fluidity of the bilayer lipids caused by a condensing effect of the hormone. The latter possibility seems unlikely, however, in light of the fact that ABA is known to increase the permeability of membranes to electrolytes (Stillwell and Hester, 1984; Harkers et al., 1985). From these observations we hypothesize that the three polar groups present on ABA introduce a certain amount of water into adjacent regions of the bilayer. We further suggest the possible existence of an alternative conformation for ABA inside the membrane as shown in Fig. 7 (denoted "alternate conformation"), in which the three polar groups are aligned close by in a linear array. In this conformation, the polar groups could form a hydrophilic, channel-like surface normal to the bilayer plane that allows for facile penetration of water molecules along the length of the hormone, thereby exposing adjacent lipid surfaces to increased interaction with water. This could explain the

overall drop in entropy upon transfer of ABA from buffer to the membrane. This effect would, however, be due to the unique structure of the hormone and would contrast with the more general mechanism suggested by Seelig and co-workers (Seelig and Ganz, 1991) from rebinding of water due to the spacing of lipid molecules during solute intercalation.

The measured enthalpy for ABA transfer (-22.6 kJ/mol) matches reasonably well with the energy of a single hydrogen bond (Atkins, 1990). A protonated carboxyl group, a hydroxyl group, and a keto group on ABA (see Fig. 1) are all within reach of the lipid polar headgroups and may be involved in hydrogen bonding. On the other hand, Wimley and White (1993) have suggested dipolar interactions as a possible source for larger enthalpic contributions. Conclusive proof of ABA-lipid hydrogen bonds would require more detailed information on the location of ABA with regard to the polar groups on the lipids than can be obtained from the DSC technique employed here.

Location of ABA in di-saturated PC bilayers

Knowing the site of solute location in a membrane is essential in determining the nature of membrane-solute interactions. Outward location of a solute within a membrane is frequently accompanied by H-bonding to the lipid headgroups, whereas deeper penetration of the solute into the membrane hydrophobic interior is manifested by strong hydrophobic interactions. The early work of Jain (Jain and Wu, 1977) is frequently cited for determination of the membrane location of solutes and is based on characteristic changes in phase transitions profiles. This work describes four different solute locations (labeled *A–D* in Table 2), each of which is associated with characteristic changes in the lipid

transition profile. More recent work, however, has shown that this simple interpretation may be insufficient. For example, the appearance of a second new solute-induced peak, which Jain correlates with a headgroup interaction and hence a *D* profile, can also be interpreted as resulting from lateral phase separation. Furthermore, Jain's *C* profiles, which are characteristic of short-chain alcohols, are interpreted as a preferential location of the solute within the lower methylene region of the bilayer. More recent evidence, however, indicates that short-chain alcohols may actually locate to the outer region of the bilayer (Westh and Trandum, 1999). To clarify this possible discrepancy, we compared our DSC results on the membrane location of ABA in Table 2 to hormone partitioning into organic solvents whose *DK* values mimic different regions of the bilayer. Octanol and decane, whose *DK* values mimic the outer versus interior parts of the membrane, respectively, resulted in partition coefficients (*P*) of 300 and 3.3 for ABA. In comparison, our experimental values for partitioning of ABA into bilayers range from 1280 for DiC₁₄PC to 470 for DiC₁₉PC, suggesting an external location of ABA. The changes in our DSC transition profiles largely follow the *A* pattern described by Jain (Jain and Wu, 1977) and support partitioning of ABA into the upper methylene region of the PC hydrocarbon tails. We therefore suggest that the hormone is partially embedded within the glycerol and headgroup regions, but also penetrates into the more hydrophobic portion of the fatty acid tails as diagramed in Fig. 1. This mode of insertion would also allow for substantial H-bond formation between ABA and PC, which could contribute to the large negative enthalpy of transfer discussed above. A similar location for ABA within the membrane was previously suggested by Burner (1993), who aligned the

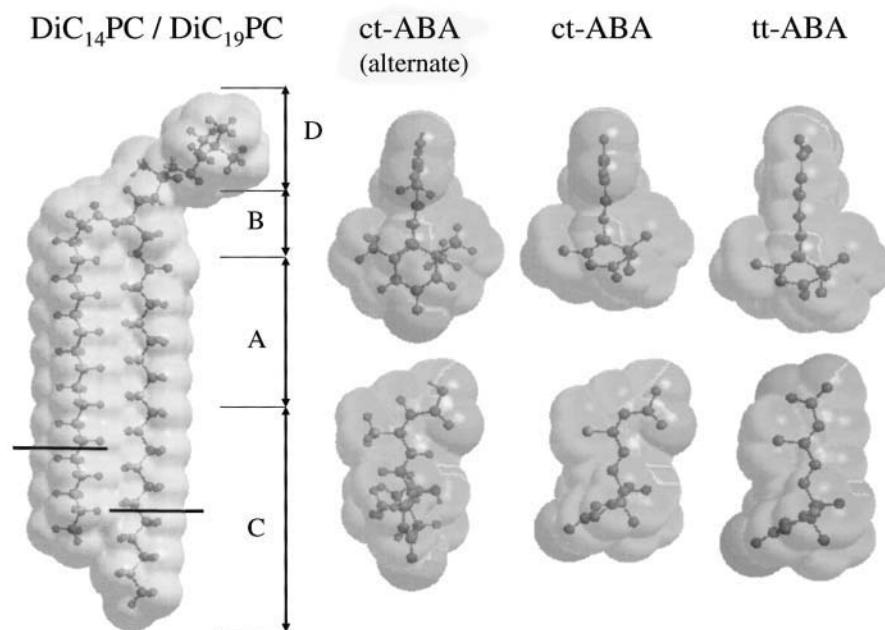


FIGURE 7 Three-dimensional structures of the phosphatidylcholines and ABA-isomers used in our experiments. Column 1 shows the shortest and longest lipid used in the experiments, DiC₁₄PC and DiC₁₉PC (the length of DiC₁₄PC is indicated by the horizontal line across the fatty acid tails). Columns 3 and 4 show models of the structures of ct- and tt-ABA, respectively, based on data from x-ray diffraction of the crystalline isomers (Schmalle et al., 1977; Swaminathan et al., 1976). The top and bottom row show the same model at 90° angle. Column 2 gives a suggested alternative conformation that differs from the model in column 3 in the conformation of the ring (alternate form: boat conformation; column 3: chair conformation) and allows for close proximity of the polar groups in a vertical line below each other along the long axis of the hormone. This close proximity of the hydrophilic groups is only possible in the alternate model for ct-ABA, but not tt-ABA, and may be energetically favorable inside a membrane environment.

fatty acid group of ABA with the ester group on the sn-2 position of a phospholipid.

An additional point of interest is the ABA-induced lower temperature shoulder in the PC thermograms, a phenomenon that is more pronounced in the shorter chain PCs. Formation of peak shoulders has been attributed to interaction of the solute with the lipid glycerol backbone (Jain and Wu, 1977). Although this basically agrees with our deduced membrane location for abscisic acid, the interpretation of such shoulders has to be treated with caution, as other phenomena like lateral phase separation can induce similar looking changes in DSC profiles. Further experiments to verify the origin of the observed shoulder from more structurally oriented techniques would therefore be highly interesting for comparison of this interpretation.

Differences between ct- and tt-ABA and biological significance

ABA occurs in two geometric isomers: *cis-trans* (ct)- and *trans-trans* (tt)-abscisic acid. Their structures are shown in Fig. 1. Despite the obvious similarity in structure and the UV-light-induced presence of both isomers in plants (Addicott, 1983), plants can discriminate sharply between the two isomers, as only the ct-isomer shows hormonal activity (Walton, 1983). Therefore, if effects of ABA on lipid bilayer membranes are to have any biological relevance, the two isomers must exert significant differences on these model membranes. Burner (1993) reported differences in the ability of the two ABA isomers to integrate into phospholipid monolayers, resulting in different collapse pressures. Stillwell and Hester (1984) measured a larger enhancement of erythritol permeability in small unilamellar vesicle (SUV) due to ct-ABA compared to tt-ABA, and Harkers et al. (1985) reported that tt-ABA and methyl-ABA, which also show no biological activity, were without effect on the K⁺ permeability of large unilamellar vesicle (LUV). The data presented in Fig. 6 indicate that membrane partitioning of ABA, which is responsible for enhancement in permeability (Harkers et al., 1985; Stillwell and Hester, 1984), is pH-dependent. Measured values for the pH in the vicinity of guard cells range from pH 5.5 (Pfanzen and Dietz, 1987) to 7.5

(Slovik and Hartung, 1992) in leaf cell walls. These data have to be discussed together with naturally occurring concentrations of ABA, as pH determines the concentration of protonated HABA, which is available for membrane partitioning. Measurements for the naturally occurring concentration of ABA range from 2 mM (Brinckmann et al., 1990) to 55 nM (Zhang et al., 2001), indicating that the concentrations used in the experiments discussed here fall within the upper range of reported values. Using the pH-dependent shift of PC transition temperatures in the presence of 1 mM ABA to determine surface *pKa* values, we obtained values of 5.3 for ct-ABA and 4.9 for tt-ABA. These values compare well with similar ones reported by Burner (1993). Using Henderson-Hasselbalch and a subphase pH of 4.8, the difference of 0.4 *pKa* units corresponds to a 1.4-fold higher membrane concentration of the protonated form of ct- relative to tt-ABA. It should be noted, however, that the sigmoidal nature of the *pKa* curves implies a pH dependence for the ratio of the surface concentration of the two isomers as demonstrated by the vertical bars in Fig. 5 A: protonated tt-ABA has an ~1.9-fold lower surface concentration than does the ct-isomer at a subphase pH of 5.5. This means that under conditions of increasing pH, the difference in surface concentration between the two isomers increases as shown in Table 3. It is interesting to note in this regard that the response of plants to drought stress in the form of a root-to-shoot signal includes an increase in apoplastic pH by up to one unit as well as an ~10-fold increase in apoplastic ABA concentration (Hartung and Radin, 1989). Together with the Henderson-Hasselbalch equation, this requires that the overall concentration of the protonated ABA species remains largely the same, while the ratios of the surface concentration of the protonated species shift slightly in favor of the biologically active (ct-ABA) isomer. Combining the difference in surface *pKa* values and partition coefficients, and assuming the same total subphase concentration for both isomers, an ~1.3-fold higher ratio of ct- to tt-ABA would reside within the membrane at pH 6.5 compared to pH 5.5. In other words, the relative concentration of membrane-bound ct-ABA at pH 6.5 is ~4.5 times higher than tt-ABA, compared to the ~3.6-fold higher membrane concentration of the ct to tt-isomer at pH 5.5.

TABLE 3 Change in subphase and membrane concentration of ct- and tt-ABA with pH

	pH 4.8		pH 5.5		pH 6.5		
	HABA	<i>R</i> _{1mM}	HABA	<i>R</i> _{1mM}	HABA	<i>R</i> _{1mM}	<i>R</i> _{10mM}
ct-ABA <i>pKa</i> 5.3	0.76	1/56	0.39	1/112	0.059	1/730	1/73
Ratio ct- to tt-ABA	1.4	2.6	1.9	3.6	2.4	4.5	4.5
tt-ABA <i>pKa</i> 4.9	0.56	1/144	0.20	1/400	0.024	1/3300	1/330

Columns marked *HABA* give the aqueous concentration of each protonated isomer on the membrane surface using the obtained surface *pKa*'s in the Henderson-Hasselbalch equation for a total buffer concentration of protonated and dissociated ABA of 1 mM. *R*_{1mM} is the membrane concentration obtained for the partition coefficients of ct- and tt-ABA into DMPC using the subphase concentration in the corresponding *A*-columns. *R*_{10mM} gives the membrane concentration for a tenfold increase in ABA concentration as seen in vivo as part of the root-to-shoot signal under conditions of drought. The second row gives the ratio of the concentrations of protonated ct- to tt-ABA listed in the first and third lines.

Published differences in membrane-directed effects for the ABA isomers such as increased solute efflux or fusogenicity (Harkers et al., 1985; Stillwell and Hester, 1984; Stillwell et al., 1988) typically show 50–60% lower efficiency of tt-compared to ct-ABA. This is in agreement with the ~2.6-fold difference in membrane concentration between the isomers at pH 4.8 reported here. Since in vivo experiments show that tt-ABA has only 2–5% of the physiological activity of ct-ABA (Walton, 1983), the difference we report in surface pK_a 's and partition coefficients for the ABA isomers do not fully account for their marked differences in physiological activity.

The significant difference in biological activity for the two ABA isomers may reside in their three-dimensional structures. While both isomers display a highly symmetric cross-shaped structure, it is only for the S-ct-isomer that the three polar groups can be aligned in close proximity on one side of the hormone (Fig. 7). Thus, ct-ABA will have a polar ridge on one side of the hormone that is missing in the S-tt-isomer. This holds even more for the biologically inactive R-enantiomers, which differ in the orientation of the side chain and hydroxyl group at the ring C₁-atom. The difference in the distribution of the polar groups on surface of the geometric isomers suggests the possibility of different entropic and enthalpic contributions to the energy of transfer for tt-ABA compared to ct-ABA. Proof of this will require further experimentation.

In summary, our experiments demonstrate the potential of ABA to interact with membranes, a process that favors the biologically active isomer over the inactive isomer. Although the membrane-based differences between the isomers discussed here cannot fully account for the difference in biological activity, they emphasize nature's choice for ct-ABA as the biologically active isomer. As the primary site of action is undisputedly the plasma membrane itself and no ABA receptor has been found, it seems reasonable to suggest that membrane interaction may play a role in the so far unspecified ABA mechanism of action. This holds, irrespective of whether this mechanism involves membrane uptake before receptor interaction or a direct effect of the hormone on the pure lipid phase itself. In this regard, the suggested differences in possible membrane conformations for the different isomers of the hormone as well as the contribution of pH changes favoring the ct-isomer have to be kept in mind for future research.

We thank Dr. R. Haak for helpful discussion and advice during preparation of this manuscript.

REFERENCES

- Addicott, F. T. 1983. *Abscisic Acid*. Praeger, New York.
- Assmann, S. M., and K. Shimazaki. 1999. The multisensory guard cell: Stomatal responses to blue light and abscisic acid. *Plant Physiol.* 119:809–815.
- Atkins, P. W. 1990. *Physical Chemistry*. 4th ed. W. H. Freeman and Company, New York.
- Bach, D. 1986. The effect of plant hormone abscisic acid on model membranes—differential scanning calorimetry and planar bilayer membranes investigations. *Biochim. Biophys. Acta.* 863:313–317.
- Burner, H. 1993. Wechselwirkungen organischer molekule mit modelsystemen. Ph.D. thesis. University of Wurzburg, Germany.
- Burner, H., R. Benz, H. Gimmmler, W. Hartung, and W. Stillwell. 1993. Abscisic acid-lipid interactions: A phospholipid monolayer study. *Biochim. Biophys. Acta.* 1150:165–172.
- Cantor, R. S. 1997. The lateral pressure profile in membranes: A physical mechanism of general anesthesia. *Biochemistry.* 36:2339–2344.
- Daeter, W., and W. Hartung. 1993. The permeability of the epidermal plasma membrane of barley leaves to abscisic acid. *Planta.* 19:41–47.
- DeYoung, L. R., and K. A. Dill. 1988. Solute partitioning into lipid bilayer membranes. *Biochemistry.* 27:5281–5289.
- DeYoung, L. R., and K. A. Dill. 1990. Partitioning of nonpolar solutes into bilayers and amorphous n-alkanes. *J. Phys. Chem.* 94:801–809.
- Diamond, J. M., and Y. Katz. 1974. Interpretation of nonelectrolyte partition coefficients between dimyristoyl lecithin and water. *J. Membr. Biol.* 17:121–154.
- Finkelstein, A. 1976. Water and nonelectrolyte permeability of lipid bilayer membranes. *J. Gen. Physiol.* 68:127–135.
- Gennis, R. B. 1989. *Biomembranes*. Springer-Verlag, New York.
- Harkers, C., W. Hartung, and H. Gimmmler. 1985. Abscisic acid mediated K⁺-efflux from large unilamellar liposomes. *J. Plant Physiol.* 122:385–394.
- Hartung, W., and J. W. Radin. 1989. Abscisic acid in the mesophyll apoplast and in the root xylem sap of water-stressed plants: The significance of pH gradients. *Curr. Top. Plant Biochem. Physiol.* 8:110–124.
- Heldt, H. W. 1997. *Plant Biochemistry and Molecular Biology*. Oxford University Press, Oxford, UK.
- Hill, M. W. 1974. The effect of anaesthetic-like molecules on the phase transition in smectic mesophases of dipalmitoyllecithin I: The normal alcohol up to C=9 and three inhalation anaesthetics. *Biochim. Biophys. Acta.* 356:117–124.
- Huang, C., and T. J. McIntosh. 1997. Probing the ethanol-induced chain interdigitations in gel-state bilayers of mixed chain phosphatidylcholines. *Biophys. J.* 72:2702–2709.
- Jain, M. K., and N. M. Wu. 1977. Effect of small molecules on the dipalmitoyl lecithin liposomal bilayer. *J. Membr. Biol.* 34:157–201.
- Jorgensen, K. 1995. Calorimetric detection of a submain transition in long-chain phosphatidylcholine lipid bilayers. *Biochim. Biophys. Acta.* 1240:111–114.
- Kamaya, H., S. Kaneshina, and I. Ueda. 1981. Partition equilibrium of inhalation anesthetics and alcohols between water and membranes of phospholipids with varying acyl chain lengths. *Biochim. Biophys. Acta.* 646:135–142.
- Lee, A. G. 1977. Lipid phase transitions and phase diagrams. II. Mixtures involving lipids. *Biochim. Biophys. Acta.* 472:285–344.
- Lee, A. G., K. A. Dalton, R. C. Duggleby, J. M. East, and A. P. Starling. 1995. Lipid structure and Ca²⁺-ATPase function. *Biosci. Rep.* 15: 289–298.
- Lide, D. R. 2001. *Handbook of Chemistry and Physics*. 82nd ed. CRC Press, Ohio. E57–E58.
- Lohner, K. 1991. Effects of small organic molecules on phospholipid phase transitions. *Chem. Phys. Lipids.* 57:341–362.
- Mabrey, S., and J. M. Sturtevant. 1976. Investigation of phase transitions of lipids and lipid mixtures by sensitivity differential scanning calorimetry. *Proc. Natl. Acad. Sci. USA.* 73:3862–3866.
- Mapelli, S., and P. Rocchi. 1983. Separation and quantification of abscisic acid and its metabolites by high performance liquid chromatography. *Ann. Bot.* 52:407–409.

- McElhaney, R. M. 1986. Differential scanning calorimetric studies of lipid-protein interactions in model membrane systems. *Biochim. Biophys. Acta*. 864:361–421.
- Muller, H.-J., M. Luxnat, and H.-J. Galla. 1986. Lateral diffusion of small solutes and partition of amphipaths in defect structures of lipid bilayers. *Biochim. Biophys. Acta*. 856:283–289.
- Overton, E. 1901. Studien Über der Narkose. Fischer, Jena, Germany.
- Pfanz, H., and K.-J. Dietz. 1987. A fluorescence method for the determination of the apoplastic proton concentration in intact leaf tissues. *J. Plant Physiol.* 129:41–48.
- Pressl, K., K. Jorgensen, and P. Lagner. 1997. Characterization of the submain transition in distearoylphosphatidylcholine studied by simultaneous small- and wide-angle x-ray diffraction. *Biochim. Biophys. Acta*. 1325:1–7.
- Raudino, A., and D. Mauzerall. 1986. Dielectric properties of the polar head group region of zwitterionic lipid bilayers. *Biophys. J.* 50:441–449.
- Rowe, E. S. 1983. Lipid chain length and temperature dependence of ethanol-phosphatidylcholine interactions. *Biochemistry*. 22:3299–3305.
- Rowe, E. S., F. Zhang, T. W. Leung, J. S. Parr, and P. T. Guy. 1998. Thermodynamics of membrane partitioning for a series of n-alcohols determined by titration calorimetry: Role of hydrophobic effects. *Biochemistry*. 37:2430–2440.
- Sarmiento, A. B., M. C. Pedrosa de Lima, and C. R. Oliveira. 1993. Partition of dopamine antagonists into synthetic lipid bilayers: the effect of membrane structure and composition. *J. Pharm. Pharmacol.* 45:601–605.
- Schmalle, H. W., K. H. Klaska, and O. Jarchow. 1977. The crystal and molecular structure of (R,S)-*cis,trans*-abscisic acid: 5-(1-hydroxy-2,6,6-trimethyl-4-oxo-2-cyclohexen-1-yl)-3-methyl-2,4-pentadienoic acid. *Acta Crystallogr.* B33:2218–2224.
- Seelig, J., and P. Ganz. 1991. Nonclassical hydrophobic effect in membrane binding equilibria. *Biochemistry*. 30:9354–9359.
- Shripathi, V., G. S. Swamy, and K. S. Chandrasekhar. 1997. Microviscosity of cucumber (*Cucumis sativus* L.) fruit protoplast membranes is altered by triacontanol and abscisic acid. *Biochim. Biophys. Acta*. 1323:263–271.
- Slovik, S., and W. Hartung. 1992. Compartmental distribution and redistribution of abscisic acid in intact leaves. III. Analysis of the stress-signal chain. *Planta*. 187:37–47.
- Stillwell, W., and P. Hester. 1984. Abscisic acid increases membrane permeability by interacting with phosphatidylethanolamine. *Biochemistry*. 23:2187–2192.
- Stillwell, W., B. Brengle, and S. R. Wassall. 1988. Abscisic acid enhances aggregation and fusion of phospholipid vesicles. *Biochem. Biophys. Res. Commun.* 156:511–516.
- Swaminathan, P., J. Vijayalakshmi, and R. Srinivasan. 1976. Molecular structure, symmetry and conformation. XVI. The crystal and molecular structure of (RS)-abscisic acid. *Acta Crystallogr. B*. 32:2351–2354.
- Tanford, C. 1980. Chapter 3. *In* The Hydrophobic Effect, 2nd ed. Wiley & Sons, Toronto, Canada.
- Walton, D. C. 1983. Structure activity relationships of abscisic acid analogs and metabolites. *In* Abscisic Acid. F.T. Addicott, editor. Praeger, New York. 113–146.
- Westh, P., and C. Trandum. 1999. Thermodynamics of alcohol-lipid bilayer interactions: Application of a binding model. *Biochim. Biophys. Acta*. 1421:261–272.
- Wimley, W. C., and S. H. White. 1993. Membrane partitioning: Distinguishing bilayer effects from the hydrophobic effect. *Biochemistry*. 32:6307–6312.
- Xiang, T. X., Y. Xu, and B. D. Anderson. 1990. The barrier domain for solute permeation varies with lipid bilayer phase structure. *J. Membr. Biol.* 165:77–90.
- Xiang, T. X., Y. Xu, and B. D. Anderson. 1994. The relationship between permeant size and permeability in lipid bilayer membranes. *J. Membr. Biol.* 140:111–112.
- Zhang, S. Q., W. H. Outlaw, Jr., and K. Aghoram. 2001. Relationship between changes in the guard cell abscisic-acid content and other stress-related physiological parameters in intact plants. *J. Exp. Bot.* 52:301–308.